

Turbo-Like Beamforming Based on Tabu Search Algorithm for Millimeter-Wave Massive MIMO Systems

Xinyu Gao, Linglong Dai, Chau Yuen, and Zhaocheng Wang

Abstract—For millimeter-wave (mmWave) massive multiple-input-multiple-output (MIMO) systems, codebook-based analog beamforming (including transmit precoding and receive combining) is usually used to compensate the severe attenuation of mmWave signals. However, conventional beamforming schemes involve complicated search among predefined codebooks to find out the optimal pair of analog precoder and analog combiner. To solve this problem, by exploring the idea of turbo equalizer together with the tabu search (TS) algorithm, we propose a Turbo-like beamforming scheme based on TS, which is called Turbo-TS beamforming in this paper, to achieve near-optimal performance with low complexity. Specifically, the proposed Turbo-TS beamforming scheme is composed of the following two key components: 1) Based on the iterative information exchange between the base station (BS) and the user, we design a Turbo-like joint search scheme to find out the near-optimal pair of analog precoder and analog combiner; and 2) inspired by the idea of the TS algorithm developed in artificial intelligence, we propose a TS-based precoding/combining scheme to intelligently search the best precoder/combiner in each iteration of Turbo-like joint search with low complexity. Analysis shows that the proposed Turbo-TS beamforming can considerably reduce the searching complexity, and simulation results verify that it can achieve near-optimal performance.

Index Terms—Beamforming, massive multiple-input-multiple-output (MIMO), millimeter wave (mmWave), tabu search (TS), turbo equalizer.

I. INTRODUCTION

The integration of millimeter-wave (mmWave) and massive multiple-input-multiple-output (MIMO) is regarded as a promising technique for future fifth-generation (5G) wireless communication systems [1] since it can provide an orders of magnitude increase both in the available bandwidth and the spectral efficiency [2]. On one hand, the very short wavelength associated with mmWave enables a large antenna array to be easily installed in a small physical dimension [3]. On the other hand, the large antenna array in massive MIMO can provide a sufficient antenna gain to compensate the severe attenuation of mmWave signals due to path loss, oxygen absorption, and rainfall effect [1] as the beamforming (including transmit precoding and receive combining) technique can concentrate the signal in a narrow beam.

Manuscript received March 14, 2015; revised June 1, 2015; accepted July 23, 2015. Date of publication July 28, 2015; date of current version July 14, 2016. This work was supported in part by the International Science and Technology Cooperation Program of China under Grant 2015DFG12760; by Singapore's Agency for Science, Technology, and Research (A*STAE) Science and Engineering Research Council Project under Grant 142 02 00043; by the National Natural Science Foundation of China under Grant 61201185 and Grant 61571270; by Beijing Natural Science Foundation under Grant 4142027; and by the Foundation of Shenzhen Government. The review of this paper was coordinated by Prof. D. B. da Costa.

X. Gao, L. Dai, and Z. Wang are with the Tsinghua National Laboratory for Information Science and Technology (TNList), Department of Electronic Engineering, Tsinghua University, Beijing 100084, China (e-mail: gxy1231992@sina.com; daill@tsinghua.edu.cn; zcwang@tsinghua.edu.cn).

C. Yuen is with the SUTD-MIT International Design Centre, Singapore University of Technology and Design, Singapore 138682 (e-mail: yuenchau@sutd.edu.sg).

Color versions of one or more of the figures in this paper are available online at <http://ieeexplore.ieee.org>.

Digital Object Identifier 10.1109/TVT.2015.2461440

MmWave massive MIMO systems usually perform beamforming in the analog domain, where the transmitted signals or received signals are only controlled by the analog phase shifter (PS) network with low hardware cost [1]. Compared with traditional digital beamforming, analog beamforming can decrease the required number of expensive radio-frequency (RF) chains at both the base station (BS) and users, which is crucial to reduce the energy consumption and hardware complexity of mmWave massive MIMO systems [4]. Existing dominant analog beamforming schemes can be generally divided into two categories, i.e., the non-codebook beamforming and the codebook-based beamforming. For the non-codebook beamforming, there are already some excellent schemes. In [5]–[7], a low-complexity analog beamforming, where two PSs are employed for each entry of the beamforming matrix, is proposed to achieve the optimal performance of fully digital beamforming. However, these methods require the perfect channel state information to be acquired by the BS, which is very challenging in practice, particularly when the number of RF chains is limited [1]. By contrast, the codebook-based beamforming can obtain the optimal pair of analog precoder and analog combiner by searching the predefined codebook without knowing the exact channel. The most intuitive and optimal scheme is full-search (FS) beamforming [8]. However, its complexity exponentially increases with the number of RF chains and quantified bits of the angle of arrival (AoA) and the angle of departure (AoD). To reduce the searching complexity of codebook-based beamforming, some low-complexity schemes, such as the schemes adopted by the IEEE 802.15.3c [9] and IEEE 802.11ad [10] standards, have already been proposed. Furthermore, a multilevel codebook, together with a ping-pong searching scheme, is also proposed in [11]. These schemes can reduce the searching complexity without obvious performance loss. However, they usually involve a large number of iterations to exchange the information between the user and the BS, leading to a high overhead for practical systems.

To reduce both the searching complexity and the overhead of codebook-based beamforming, in this paper, we propose a Turbo-like beamforming scheme based on the tabu search (TS) algorithm [12] (called as Turbo-TS beamforming) with near-optimal¹ performance for mmWave massive MIMO systems. Specifically, the proposed Turbo-TS beamforming scheme is composed of the following two key components.

- 1) Based on the iterative information exchange between the BS and the user, we design a Turbo-like joint search scheme to find out the near-optimal pair of analog precoder and analog combiner.
- 2) Inspired by the TS algorithm in artificial intelligence, we develop a TS-based precoding/combining to intelligently search the best precoder/combiner in each iteration of Turbo-like joint search with low complexity.

Furthermore, the contributions of the proposed TS-based precoding/combining can be summarized in the following three aspects.

- 1) Provide the appropriate definitions of neighborhood, cost, and stopping criterion involved in TS-based precoding/combining.
- 2) Take the exact solution instead of the conventional “move” as tabu to guarantee a wider searching range.
- 3) Propose a restart method by selecting several different initial solutions uniformly distributed in the codebooks to further improve the performance.

¹Note that “near-optimal” means achieving the performance close to that of the optimal FS beamforming.

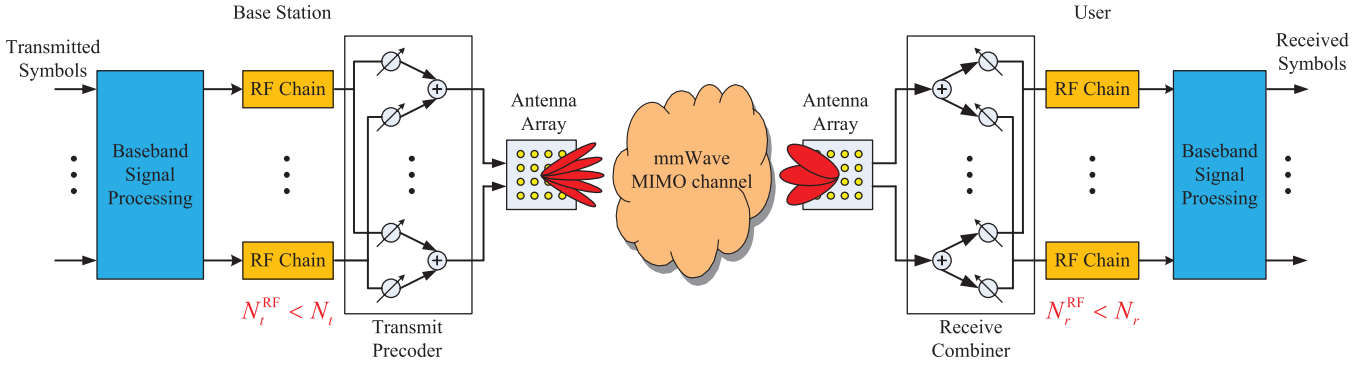


Fig. 1. Architecture of the mmWave massive MIMO system with beamforming.

It is shown that the proposed Turbo-TS beamforming can considerably reduce the searching complexity. We verify through simulations that Turbo-TS beamforming can approach the performance of FS beamforming [8].

The remainder of this paper is organized as follows. Section II briefly introduces the system model of mmWave massive MIMO. Section III specifies the proposed Turbo-TS beamforming. The simulation results of achievable rate are shown in Section IV. Finally, conclusions are drawn in Section V.

Notation: Lowercase and uppercase boldface letters denote vectors and matrices, respectively; $(\cdot)^T$, $(\cdot)^H$, $(\cdot)^{-1}$, and $\det(\cdot)$ denote the transpose, conjugate transpose, inversion, and determinant of a matrix, respectively; and $\mathbb{E}(\cdot)$ denotes the expectation. Finally, \mathbf{I}_N is the $N \times N$ identity matrix.

II. SYSTEM MODEL

We consider the mmWave massive MIMO system with beamforming, as shown in Fig. 1, where the BS employs N_t antennas and N_t^{RF} RF chains to simultaneously transmit N_s data streams to a user with N_r antennas and N_r^{RF} RF chains. To fully achieve the spatial multiplexing gain, we usually have $N_t^{\text{RF}} = N_r^{\text{RF}} = N_s$ [13]. The N_s independent transmitted data streams in the baseband first pass through N_t^{RF} RF chain to be converted into analog signals. After this, the output signals will be precoded by an $N_t \times N_t^{\text{RF}}$ analog precoder \mathbf{P}_A as $\mathbf{x} = \mathbf{P}_A \mathbf{s}$ before transmission, where \mathbf{s} is the $N_s \times 1$ transmitted signal vector subject to the normalized power $\mathbb{E}(\mathbf{s}\mathbf{s}^H) = (1/N_s)\mathbf{I}_{N_s}$. Note that the analog precoder \mathbf{P}_A is usually realized by a PS network with low hardware complexity [1], which requires that all elements of \mathbf{P}_A should satisfy $|p_{i,j}^A|^2 = 1/N_t$. Under the narrow-band block-fading massive MIMO channel [13], $N_r \times 1$ received signal vector \mathbf{r} at the user can be presented as

$$\mathbf{r} = \sqrt{\rho}\mathbf{H}\mathbf{P}_A\mathbf{s} + \mathbf{n} \quad (1)$$

where ρ is the transmitted power; $\mathbf{H} \in \mathbb{C}^{N_r \times N_t}$ denotes the channel matrix, which will be discussed in detail later in this section; and $\mathbf{n} = [n_1, \dots, n_{N_r}]^T$ is the additive white Gaussian noise vector, whose entries follow the independent and identical distribution (i.i.d.) $\mathcal{CN}(0, \sigma^2 \mathbf{I}_{N_r})$ [14].

At the user side, an $N_r \times N_r^{\text{RF}}$ analog combiner \mathbf{C}_A is employed to process the received signal vector \mathbf{r} as

$$\mathbf{y} = \mathbf{C}_A^H \mathbf{r} = \sqrt{\rho}\mathbf{C}_A^H \mathbf{H} \mathbf{P}_A \mathbf{s} + \mathbf{C}_A^H \mathbf{n} \quad (2)$$

where the elements of \mathbf{C}_A have the similar constraints as those of \mathbf{P}_A , i.e., $|c_{i,j}^A|^2 = 1/N_r$.

Due to the limited number of significant scatters and serious antenna correlation of mmWave communication [15], [16], in this paper, we

adopt the widely used geometric Saleh–Valenzuela channel model [13], where the channel matrix \mathbf{H} can be presented as

$$\mathbf{H} = \sqrt{\frac{N_t N_r}{L}} \sum_{l=1}^L \alpha_l \mathbf{f}_r(\phi_l^r) \mathbf{f}_t^H(\phi_l^t) \quad (3)$$

where L is the number of significant scatters, and we usually have $L \leq \min(N_t, N_r)$ for mmWave communication systems due to the sparse nature of scatters; $\alpha_l \in \mathbb{C}$ is the gain of the l th path including the path loss; and ϕ_l^t and ϕ_l^r are the azimuth of AoDs/AoAs of the l th path, respectively. Finally, $\mathbf{f}_t(\phi_l^t)$ and $\mathbf{f}_r(\phi_l^r)$ are the antenna array response vectors, which depend on the antenna array structure at the BS and the user. When the widely used uniform linear arrays (ULAs) are considered, we have [13]

$$\mathbf{f}_t(\phi_l^t) = \frac{1}{\sqrt{N_t}} [1, e^{jk d \sin(\phi_l^t)}, \dots, e^{j(N_t-1)k d \sin(\phi_l^t)}]^T \quad (4)$$

$$\mathbf{f}_r(\phi_l^r) = \frac{1}{\sqrt{N_r}} [1, e^{jk d \sin(\phi_l^r)}, \dots, e^{j(N_r-1)k d \sin(\phi_l^r)}]^T \quad (5)$$

where $k = (2\pi/\lambda)$, λ denotes the wavelength of the signal, and d is the antenna spacing.

III. NEAR-OPTIMAL TURBO-TABU SEARCH BEAMFORMING WITH LOW COMPLEXITY

Here, we first give a brief introduction of the codebook-based beamforming, which is widely used in mmWave massive MIMO systems. After this, a low-complexity near-optimal Turbo-TS beamforming scheme is proposed, which consists of Turbo-like joint search scheme and TS-based precoding/combining. Finally, the complexity analysis is provided to show the advantage of the proposed Turbo-TS beamforming scheme.

A. Codebook-Based Beamforming

According to the special characteristic of a mmWave channel, the beamsteering codebook [8] is widely used. Specifically, let \mathcal{F} and \mathcal{W} denote the beamsteering codebooks for the analog precoder and the analog combiner, respectively. If we use B_t^{RF} (B_r^{RF}) bits to quantify the AoD (AoA), \mathcal{F} (\mathcal{W}) will consist of all the possible analog precoder (combiner) matrices \mathbf{P}_A (\mathbf{C}_A), which can be presented as [8]

$$\mathbf{P}_A = [\mathbf{f}_t(\bar{\phi}_1^t), \mathbf{f}_t(\bar{\phi}_2^t), \dots, \mathbf{f}_t(\bar{\phi}_{N_t^{\text{RF}}}^t)] \quad (6)$$

$$\mathbf{C}_A = [\mathbf{f}_r(\bar{\phi}_1^r), \mathbf{f}_r(\bar{\phi}_2^r), \dots, \mathbf{f}_r(\bar{\phi}_{N_r^{\text{RF}}}^r)] \quad (7)$$

where the quantified AoD $\bar{\phi}_i^t$ for $i = 1, \dots, N_t^{\text{RF}}$ at the BS has $2^{B_t^{\text{RF}}}$ possible candidates, i.e., $\bar{\phi}_i^t = 2\pi n / 2^{B_t^{\text{RF}}}$ where $n \in \{1, \dots, 2^{B_t^{\text{RF}}}\}$.

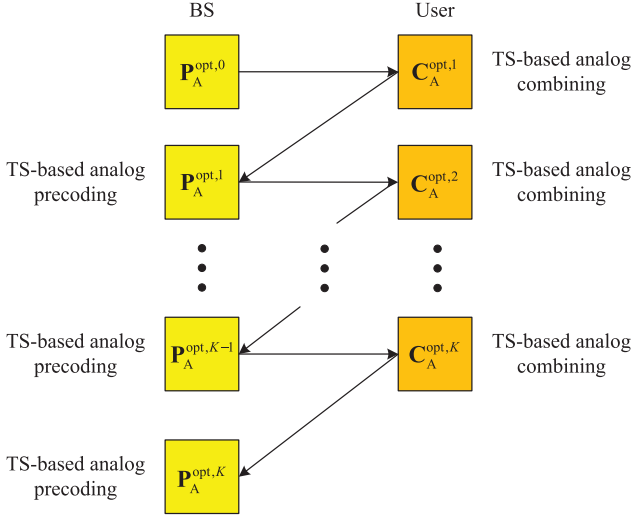


Fig. 2. Proposed Turbo-like joint search scheme.

Similarly, the quantified AoA $\bar{\phi}_j^r$ for $j = 1, \dots, N_r^{\text{RF}}$ at the user has $2^{B_r^{\text{RF}}}$ possible candidates, i.e., $\bar{\phi}_j^r = 2\pi n/2^{B_r^{\text{RF}}}$ where $n \in \{1, \dots, 2^{B_r^{\text{RF}}}\}$. Thus, the cardinalities $|\mathcal{F}|$ of \mathcal{F} and $|\mathcal{W}|$ of \mathcal{W} are $2^{B_t^{\text{RF}} \cdot N_t^{\text{RF}}}$ and $2^{B_r^{\text{RF}} \cdot N_r^{\text{RF}}}$, respectively. Then, by jointly searching \mathcal{F} and \mathcal{W} , the optimal pair of analog precoder and analog combiner can be selected by maximizing the achievable rate as [13]

$$R = \max_{\mathbf{P}_A \in \mathcal{F}, \mathbf{C}_A \in \mathcal{W}} \log_2 \left(\mathbf{I}_{N_s} + \frac{\rho}{N_s} \mathbf{R}_n^{-1} \mathbf{C}_A^H \mathbf{H} \mathbf{P}_A \mathbf{P}_A^H \mathbf{H}^H \mathbf{C}_A \right) = \max_{\mathbf{P}_A \in \mathcal{F}, \mathbf{C}_A \in \mathcal{W}} \log_2 (\varphi(\mathbf{P}_A, \mathbf{C}_A)) \quad (8)$$

where $\mathbf{R}_n = \sigma^2 \mathbf{C}_A^H \mathbf{C}_A$ presents the covariance matrix of noise after combining, and

$$\varphi(\mathbf{P}_A, \mathbf{C}_A) = \left| \mathbf{I}_{N_s} + \frac{\rho}{N_s} \mathbf{R}_n^{-1} \mathbf{C}_A^H \mathbf{H} \mathbf{P}_A \mathbf{P}_A^H \mathbf{H}^H \mathbf{C}_A \right| \quad (9)$$

is defined as the cost function. We can observe that, to obtain the optimal pair of analog precoder and analog combiner, we need to exhaustively search the codebooks \mathcal{F} and \mathcal{W} . When $N_r^{\text{RF}} = N_t^{\text{RF}} = 2$ and $B_t^{\text{RF}} = B_r^{\text{RF}} = 6$, the totally required time of search is 1.6×10^7 , which is almost impossible in practice. In this paper, we propose Turbo-TS beamforming to reduce the searching complexity. The proposed Turbo-TS beamforming is composed of two key components, i.e., Turbo-like joint search scheme and TS-based precoding/combining, which will be described in detail in Section III-B and C, respectively.

B. Turbo-Like Joint Search Scheme

Based on the idea of the information interaction in the well-known turbo equalizer, we propose a Turbo-like joint search scheme to find out the near-optimal pair of analog precoder and analog combiner, which is shown in Fig. 2. Let $\mathbf{P}_A^{\text{opt},k}$ and $\mathbf{C}_A^{\text{opt},k}$ denote the near-optimal analog precoder and analog combiner obtained in the k th iteration, respectively, where $k = 1, 2, \dots, K$, and K is the predefined maximum number of iterations. First, the BS selects an initial precoder $\mathbf{P}_A^{\text{opt},0}$, which can be an arbitrary candidate in \mathcal{F} , to transmit a training sequence to the user. Then, the user can search the best analog combiner $\mathbf{C}_A^{\text{opt},1}$. After this, the user uses $\mathbf{C}_A^{\text{opt},1}$ to transmit a training sequence to the BS, and in return, the BS can search the best analog precoder $\mathbf{P}_A^{\text{opt},1}$. We repeat such iteration for K times in a similar way as the turbo equalizer and output $\mathbf{P}_A^{\text{opt},K}$ and $\mathbf{C}_A^{\text{opt},K}$ as the final pair

of analog precoder and analog combiner, which is expected to achieve near-optimal performance, as will be verified later in Section IV. Note that, in each iteration, searching the best analog precoder (combiner) after a potential analog combiner (precoder) has been selected from the codebook \mathcal{W} (\mathcal{F}) can be realized by the proposed TS-based analog precoding/combining with low complexity, which will be described in detail next.

C. TS-Based Precoding/Combining

Here, we first focus on the process of searching the best analog precoder \mathbf{P}_A after a potential analog combiner \mathbf{C}_A has been selected. The process of searching the best analog combiner \mathbf{C}_A after a certain analog precoder \mathbf{P}_A has been selected can be derived in the similar way.

The basic idea of the proposed TS-based analog precoding can be described as follows. TS-based analog precoding starts from an initial solution, i.e., an analog precoder matrix selected from the codebook \mathcal{F} , and defines a neighborhood around it (several analog precoder matrices from \mathcal{F} based on a neighboring criterion). After this, it selects the most appropriate solution among the neighborhood as the starting point for the next iteration, even if it is not the global optimum. During the search in the neighborhood, TS attempts to escape from the local optimum by utilizing the concept of ‘‘tabu,’’ whose definition can be changed according to different criteria (e.g., convergence speed and complexity). This process will be continued until a certain stopping criterion is satisfied, and finally, the best solution among all iterations will be declared as the final solution. Next, five important aspects of the proposed TS-based precoding, including neighborhood definition, cost computation, tabu, stopping criterion, and TS algorithm, will be explained in detail as follows.

1) *Neighborhood Definition:* Note that the m th column of analog precoder \mathbf{P}_A can be presented by an index $q_m \in \{1, 2, \dots, 2^{B_t^{\text{RF}}}\}$, which corresponds to the vector $\mathbf{f}_t(2\pi q_m/2^{B_t^{\text{RF}}})$ as defined in (4) and (6). Then, an analog precoder is defined as a neighbor of \mathbf{P}_A if i) it has only one column that is different from the corresponding column in \mathbf{P}_A and ii) if the index difference between the two corresponding columns is equal to one. For example, when $N_t^{\text{RF}} = 2$ and $B_t^{\text{RF}} = 3$, for a possible analog precoder $\mathbf{P}_A = [\mathbf{f}_t(3\pi/4), \mathbf{f}_t(7\pi/4)]$, another precoder $[\mathbf{f}_t(2\pi/4), \mathbf{f}_t(7\pi/4)]$ is a neighbor of \mathbf{P}_A .

Let $\mathbf{P}_A^{(i)}$ denote the starting point in the i th iteration of the proposed TS-based analog precoding, and $\mathcal{V}(\mathbf{P}_A^{(i)}) = \{\mathbf{V}_1^{(i)}, \mathbf{V}_2^{(i)}, \dots, \mathbf{V}_{|\mathcal{V}|}^{(i)}\}$ presents the neighborhood of $\mathbf{P}_A^{(i)}$, where $|\mathcal{V}|$ is the cardinality of \mathcal{V} . According to this neighborhood definition, it is obvious that $|\mathcal{V}| = 2N_t^{\text{RF}}$. We then define that the u th neighbor in $\mathcal{V}(\mathbf{P}_A^{(i)})$ is different from $\mathbf{P}_A^{(i)}$ in the $\lceil u/2 \rceil$ th column, and the index of the corresponding column is $q_{\lceil u/2 \rceil} + (-1)^{\text{mod}(u,2)}$, where $q_{\lceil u/2 \rceil}$ is the index of this column. To avoid overflow of this definition, we set

$$1 + (-1)^{\text{mod}(u,2)} = \max(1 + (-1)^{\text{mod}(u,2)}, 1) \quad (10)$$

$$2^{B_t^{\text{RF}}} + (-1)^{\text{mod}(u,2)} = \min(2^{B_t^{\text{RF}}} + (-1)^{\text{mod}(u,2)}, 2^{B_t^{\text{RF}}}). \quad (11)$$

For example, the neighborhood of one analog precoder $\mathbf{P}_A^{(i)} = [\mathbf{f}_t(3\pi/4), \mathbf{f}_t(7\pi/4)]$ is $\mathbf{V}_1^{(i)} = [\mathbf{f}_t(2\pi/4), \mathbf{f}_t(7\pi/4)]$, $\mathbf{V}_2^{(i)} = [\mathbf{f}_t(4\pi/4), \mathbf{f}_t(7\pi/4)]$, $\mathbf{V}_3^{(i)} = [\mathbf{f}_t(3\pi/4), \mathbf{f}_t(6\pi/4)]$, and $\mathbf{V}_4^{(i)} = [\mathbf{f}_t(3\pi/4), \mathbf{f}_t(8\pi/4)]$.

2) *Cost Computation:* We define the value of the cost function $\varphi(\mathbf{P}_A, \mathbf{C}_A)$ in (9) as the reliability metric of a possible solution, i.e., a solution \mathbf{P}_A leading to a larger value of $\varphi(\mathbf{P}_A, \mathbf{C}_A)$ is a better solution. Furthermore, according to the neighborhood definition, we can observe that, once we obtain the cost of \mathbf{P}_A , we do not

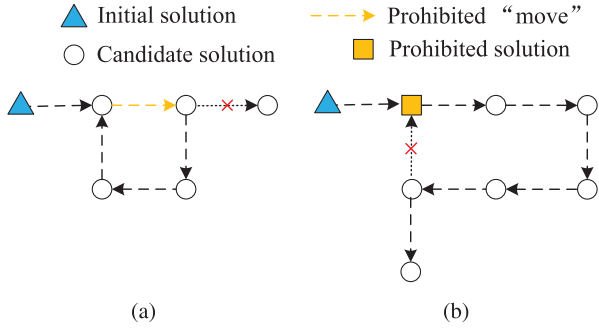


Fig. 3. Illustration of how the solution tabu can avoid one solution being searched twice. (a) Conventional “move” tabu. (b) Proposed solution tabu.

need to recompute (9) to obtain the cost of its neighborhood through information exchange between the BS and the user. This is due to the fact that the neighbor \mathbf{V}_u of \mathbf{P}_A only has the $\lceil u/2 \rceil$ th column that is different from the corresponding column in \mathbf{P}_A , and then the updated effective channel matrix $\mathbf{C}_A^H \mathbf{H} \mathbf{V}_u$ in (9) also has the $\lceil u/2 \rceil$ th column that is different from the corresponding column in the original effective channel matrix $\mathbf{C}_A^H \mathbf{H} \mathbf{P}_A$, where such difference can be easily calculated since \mathbf{P}_A and \mathbf{V}_u are known. More importantly, this special property indicates that, for the proposed TS-based analog precoding, we can only estimate the effective channel matrix $\mathbf{C}_A^H \mathbf{H} \mathbf{P}_A$ of size $N_r^{\text{RF}} \times N_t^{\text{RF}}$ through time-domain and/or frequency-domain training sequence [17], [18], whose dimension is much lower than the original dimension $N_r \times N_t$ of the channel matrix \mathbf{H} .

3) *Tabu*: In the conventional TS algorithm [12], the tabu is usually defined as the “move,” which can be regarded as the direction from one solution to another solution for the analog precoding problem. The “move” can be denoted by (a, b) , where $a = 1, \dots, N_t^{\text{RF}}$ denotes that the a th column of the original solution is different from that of the current solution, and $b \in \{-1, 1\}$ means the changed index of this particular column from the original solution to the current solution. Considering this example, the “move” (direction) from $[\mathbf{f}_t(3\pi/4), \mathbf{f}_t(7\pi/4)]$ to $[\mathbf{f}_t(2\pi/4), \mathbf{f}_t(7\pi/4)]$ can be written as $(1, -1)$. Regarding the “move” as tabu can save storage of the tabu list since it only requires a tabu list \mathbf{t} of size $2N_t^{\text{RF}} \times 1$, whose element takes the value from $\{0, 1\}$ to indicate whether a move is tabu or not (i.e., 1 is tabu, and 0 is unconstrained). However, as shown in Fig. 3(a), this method may lead to the unexpected fact that one solution will be searched twice, and the cost function of the same neighborhood will be computed again. To solve this problem, we propose to take the exact solution as tabu. Specifically, let $p = 1, 2, \dots, 2^{B_t^{\text{RF}} \cdot N_t^{\text{RF}}}$ present the index of a candidate of the analog precoder (solution) out of \mathcal{F} with $2^{B_t^{\text{RF}} \cdot N_t^{\text{RF}}}$ possible candidates. In particular, p can be calculated by each column index q_m ($1 \leq q_m \leq N_t^{\text{RF}}$)² of this analog precoder as

$$p = \sum_{m=1}^{N_t^{\text{RF}}} (q_m - 1) \left(2^{B_t^{\text{RF}}} \right)^{N_t^{\text{RF}} - m} + 1. \quad (12)$$

For example, when $B_t^{\text{RF}} = 3$ and $N_t^{\text{RF}} = 2$, if an analog precoder has the column indexes $\{2, 7\}$, then the index of this analog precoder in \mathcal{F} is $p = 15$ according to (12). This way, our method can efficiently avoid one solution being searched twice, and therefore, a wider searching range can be achieved, as shown in Fig. 3(b). Note that the only

²It is worth pointing out that to fully achieve the spatial multiplexing gain, the column index q_m should be different for different RF chains, i.e., $q_1 \neq q_2 \neq \dots \neq q_{N_r^{\text{RF}}}$. All the possible precoder/combiner matrices that do not obey this constraint will be declared as “tabu” to avoid being searched.

TABLE I
COMPLEXITY COMPARISON

	FS beamforming [8]	Turbo-TS beamforming	Complexity ratio (TS/FS)
$B_t^{\text{RF}} = B_r^{\text{RF}} = 4$	57600	16000	27.8 %
$B_t^{\text{RF}} = B_r^{\text{RF}} = 5$	984064	64000	6.5 %
$B_t^{\text{RF}} = B_r^{\text{RF}} = 6$	16257024	480000	2.9 %

cost of our method is the increased storage size of the tabu list \mathbf{t} from $2N_t^{\text{RF}}$ to $2^{B_t^{\text{RF}} \cdot N_t^{\text{RF}}}$.

4) *Stopping Criterion*: We define flag as a parameter to indicate how long (in terms of the number of iterations) the global optimal solution has not been updated. This means that, in the current iteration, if a suboptimal solution is selected as the starting point for the next iteration, we have $\text{flag} = \text{flag} + 1$; otherwise, if the global optimal solution is selected, we set $\text{flag} = 0$. Based on this mechanism, TS-based analog precoding will be terminated when either of the following two conditions is satisfied: i) The total number of iterations reaches the predefined maximum number of iterations max_iter , or ii) the number of iterations for the global optimal solution not being updated reaches the predefined maximum value max_len , i.e., $\text{flag} = \text{max_len}$. Note that we usually set $\text{max_len} < \text{max_iter}$, which means that, if TS-based analog precoding has already found the optimal solution at the beginning, all the starting points in following iterations will be suboptimal; thus, we do not need to wait max_iter iterations. Therefore, the average searching complexity can be reduced further.

5) *TS Algorithm*: Let $\mathbf{G}^{(i)}$ denote the analog precoder achieving the maximum cost function (9) that has been found until the i th iteration. TS-based analog precoding starts with the initial solution $\mathbf{P}_A^{(0)}$. Note that, to improve the performance of TS-based analog precoding, we can select M different initial solutions uniformly distributed in \mathcal{F} to start TS-based analog precoding M times; then, the best one out of M obtained solutions will be declared as the final analog precoder. For each initial solution, we set $\mathbf{G}^{(0)} = \mathbf{P}_A^{(0)}$, $\text{flag} = 0$. In addition, all the elements of the tabu list \mathbf{t} are set as zero. Considering the i th iteration, TS-based analog precoding executes as follows.

Step 1: Compute the cost function (9) of the $2N_t^{\text{RF}}$ neighbors of $\mathbf{P}_A^{(i)}$ given the effective channel matrix $\mathbf{C}_A^H \mathbf{H} \mathbf{P}_A^{(i)}$. Let

$$\mathbf{V}^1 = \arg \max_{1 \leq u \leq 2N_t^{\text{RF}}} \varphi(\mathbf{V}_u, \mathbf{C}_A). \quad (13)$$

Calculate the index p^1 of \mathbf{V}^1 in \mathcal{F} according to (12). Then, \mathbf{V}^1 will be selected as the starting point for the next iteration when either of the following two conditions is satisfied:

$$\varphi(\mathbf{V}^1, \mathbf{C}_A) > \varphi(\mathbf{G}^{(i)}, \mathbf{C}_A) \quad (14)$$

$$\mathbf{t}(p^1) = 0. \quad (15)$$

If \mathbf{V}^1 cannot be selected, we find the second best solution as

$$\mathbf{V}^2 = \arg \max_{\substack{1 \leq u \leq 2N_t^{\text{RF}} \\ \mathbf{V}_u \neq \mathbf{V}^1}} \varphi(\mathbf{V}_u, \mathbf{C}_A). \quad (16)$$

Then, we decide whether \mathbf{V}^2 can be selected by checking (14) and (15). This procedure will be continued until one solution \mathbf{V}^l is selected as the starting point for the next iteration. Note that, if there is no solution satisfying (14) and (15), all the corresponding elements of the tabu list \mathbf{t} will be set to zero, and the same procedure will be repeated.

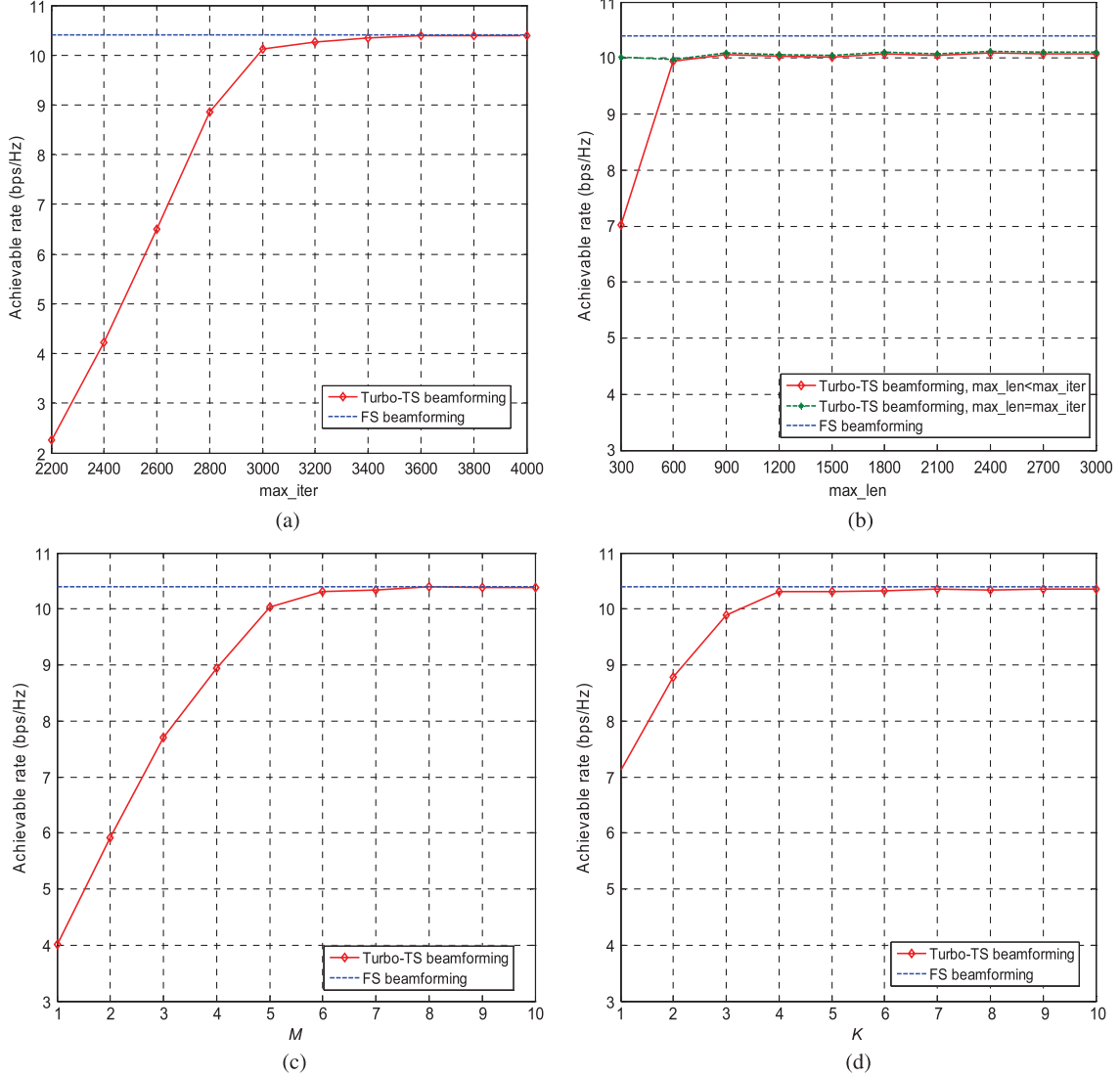


Fig. 4. Achievable rate of Turbo-TS beamforming against different parameters. (a) max_iter. (b) max_len. (c) M . (d) K .

Step 2: After a solution has been selected as the starting point, i.e., $\mathbf{P}_A^{(i+1)} = \mathbf{V}'$, we set

$$\begin{cases} \mathbf{t}(p') = 0, \mathbf{G}^{(i+1)} = \mathbf{P}_A^{(i+1)}, \\ \text{if } \varphi(\mathbf{P}_A^{(i+1)}, \mathbf{C}_A) > \varphi(\mathbf{G}^{(i)}, \mathbf{C}_A), \\ \mathbf{t}(p') = 1, \mathbf{G}^{(i+1)} = \mathbf{G}^{(i)}, \\ \text{if } \varphi(\mathbf{P}_A^{(i+1)}, \mathbf{C}_A) \leq \varphi(\mathbf{G}^{(i)}, \mathbf{C}_A). \end{cases} \quad (17)$$

TS-based analog precoding will be terminated in *Step 2* and output $\mathbf{G}^{(i+1)}$ as the final solution if the stopping criterion is satisfied. Otherwise, it will go back to *Step 1*, and repeat the procedure until it satisfies the stopping criterion.

It is worth pointing out that searching the near-optimal analog combiner \mathbf{C}_A after a certain analog precoder \mathbf{P}_A has been selected can be also solved by the similar procedure previously described, where the definitions such as neighborhood should be changed accordingly to search the near-optimal analog combiner \mathbf{C}_A .

D. Complexity Analysis

Here, we provide the complexity comparison between the proposed Turbo-TS beamforming and the conventional FS beamforming. It is

worth pointing out that, although the proposed Turbo-TS beamforming requires some extra information exchange between the BS and the UE (K times of iterations) as discussed in Section III-B, the corresponding overhead is trivial compared with the searching complexity since K is usually small (e.g., $K = 4$ as will be verified by simulation results). Therefore, here, we evaluate the complexity as the total number of solutions needed to be searched. It is obvious that the searching complexity of FS beamforming C_{FS} is

$$C_{\text{FS}} = \binom{N_t^{\text{RF}}}{2^{B_t^{\text{RF}}}} \times \binom{N_r^{\text{RF}}}{2^{B_r^{\text{RF}}}}. \quad (18)$$

By contrast, the searching complexity of the proposed Turbo-TS beamforming C_{TS} is

$$C_{\text{TS}} = (2N_t^{\text{RF}} \cdot \max_iter + 2N_r^{\text{RF}} \cdot \max_iter) MK. \quad (19)$$

Comparing (18) and (19), we can observe that the complexity of Turbo-TS beamforming is linear with N_t^{RF} and N_r^{RF} , and it is independent of B_t^{RF} and B_r^{RF} , which indicates that Turbo-TS beamforming enjoys much lower complexity than FS beamforming. Table I shows the comparison of the searching complexity between Turbo-TS beamforming and FS beamforming when the numbers of RF chains

at the BS and the user are $N_t^{\text{RF}} = N_r^{\text{RF}} = 2$, where three cases are considered.

- 1) For $B_t^{\text{RF}} = B_r^{\text{RF}} = 4$, we set $\text{max_iter} = 500$ and $\text{max_len} = 100$ and uniformly select $M = 1$ different initial solutions to initiate the TS-based precoding/combining.
- 2) For $B_t^{\text{RF}} = B_r^{\text{RF}} = 5$, we set $\text{max_iter} = 1000$, $\text{max_len} = 200$, and $M = 2$.
- 3) For $B_t^{\text{RF}} = B_r^{\text{RF}} = 6$, we set $\text{max_iter} = 3000$, $\text{max_len} = 600$, and $M = 5$.

In addition, for all these cases, we set the total number of iterations $K = 4$ for the Turbo-like joint search scheme. In Table I, we can observe that the proposed Turbo-TS beamforming scheme has much lower searching complexity than the conventional FS beamforming, e.g., when $B_t^{\text{RF}} = B_r^{\text{RF}} = 6$, the searching complexity of Turbo-TS beamforming is only 2.1% of that of FS beamforming.

IV. SIMULATION RESULTS

We evaluate the performance of the proposed Turbo-TS beamforming in terms of the achievable rate. Here, we also provide the performance of the recently proposed beam steering scheme [19] with continuous angles as the benchmark for comparison since it can be regarded as the upper bound of the proposed Turbo-TS beamforming with quantified AoAs/AoDs. The system parameters for the simulation are described as follows: The carrier frequency is set as 28 GHz; We generate the channel matrix according to the channel model [13] described in Section II. The AoAs/AoDs are assumed to follow the uniform distribution within $[0, \pi]$. The complex gain α_l of the l th path follows $\alpha_l \sim \mathcal{CN}(0, 1)$, and the total number of scattering propagation paths is set as $L = 3$. Both the transmit and receive antenna arrays are ULAs with antenna spacing $d = \lambda/2$. Three cases of quantified bits per AoA/AoD, i.e., $B_t^{\text{RF}} = B_r^{\text{RF}} = 4$, $B_t^{\text{RF}} = B_r^{\text{RF}} = 5$, and $B_t^{\text{RF}} = B_r^{\text{RF}} = 6$, are evaluated. SNR is defined as ρ/σ^2 . Additionally, the parameters used for the proposed TS-based precoding/combining are the same as those in Section III-D.

At first, we provide the achievable rate performance of Turbo-TS beamforming against different parameters to explain why we choose these values as listed in Section III-D. Fig. 4 shows an example when $N_r \times N_t = 16 \times 64$, $N_r^{\text{RF}} = N_t^{\text{RF}} = N_s = 2$, $B_t^{\text{RF}} = B_r^{\text{RF}} = 6$, and SNR = 0 dB. We can observe that, when $\text{max_iter} = 3000$ [see Fig. 4(a)], $\text{max_len} = 600$ [see Fig. 4(b)], $M = 5$ [see Fig. 4(c)], and $K = 4$ [see Fig. 4(d)], the proposed Turbo-TS beamforming can achieve more than 90% of the rate of FS beamforming, which verifies the rationality of our selection.

Fig. 5 shows the achievable rate comparison between the conventional FS beamforming and the proposed Turbo-TS beamforming for an $N_r \times N_t = 16 \times 64$ mmWave massive MIMO system with $N_r^{\text{RF}} = N_t^{\text{RF}} = N_s = 2$. We can observe that Turbo-TS beamforming can approach the achievable rate of FS beamforming without obvious performance loss. For example, when $B_t^{\text{RF}} = B_r^{\text{RF}} = 4$ and SNR = 0 dB, the rate achieved by Turbo-TS beamforming is 7 bits/s/Hz, which is quite close to 7.2 bits/s/Hz achieved by FS beamforming. When the number of quantified bits per AoA/AoD increases, both Turbo-TS beamforming and FS beamforming can achieve better performance close to the beam steering scheme with continuous AoAs/AoDs [19]. Meanwhile, Turbo-TS beamforming can still guarantee satisfying performance quite close to FS beamforming. Considering the considerably reduced searching complexity of Turbo-TS beamforming, we can conclude that the proposed Turbo-TS beamforming achieves a much better tradeoff between performance and complexity.

Fig. 6 shows the achievable rate comparison for an $N_r \times N_t = 32 \times 128$ mmWave massive MIMO system, where the number of

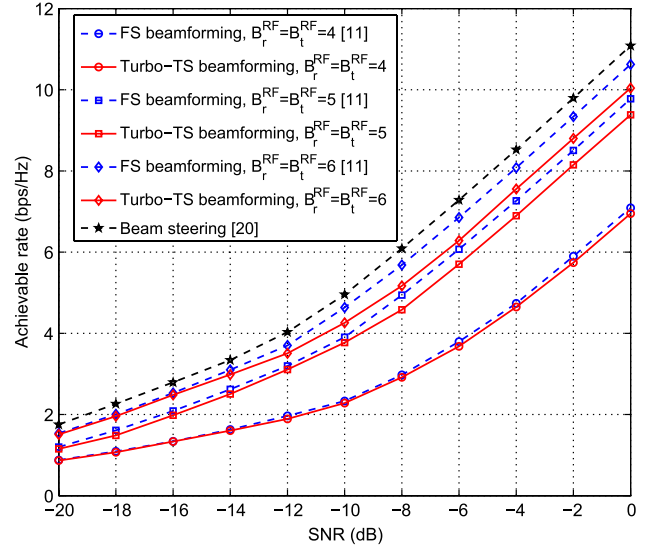


Fig. 5. Achievable rate comparison for an $N_r \times N_t = 16 \times 64$ mmWave massive MIMO system with $N_r^{\text{RF}} = N_t^{\text{RF}} = N_s = 2$.

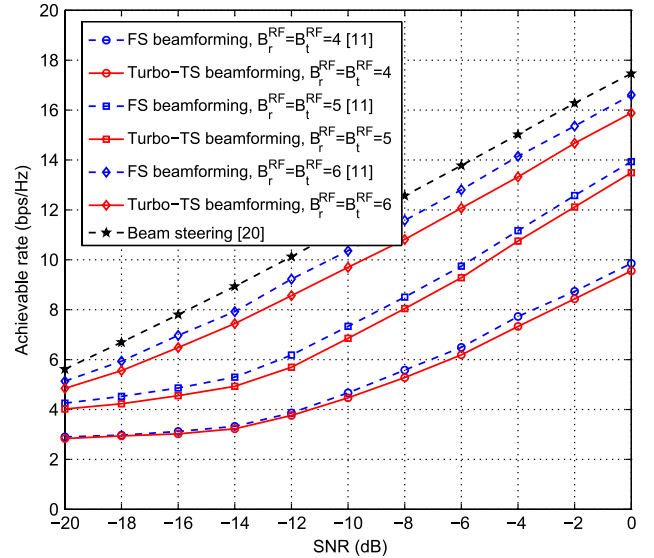


Fig. 6. Achievable rate comparison for an $N_r \times N_t = 32 \times 128$ mmWave massive MIMO system with $N_r^{\text{RF}} = N_t^{\text{RF}} = N_s = 2$.

RF chains is still set as $N_r^{\text{RF}} = N_t^{\text{RF}} = N_s = 2$. In Fig. 6, we can observe similar trends as those in Fig. 5. More importantly, comparing Figs. 5 and 6, we can find that the performance of the proposed Turbo-TS beamforming can be improved by increasing the number of low-cost antennas instead of increasing the number of expensive RF chains. For example, when $N_r \times N_t = 16 \times 64$, $B_t^{\text{RF}} = B_r^{\text{RF}} = 6$, and SNR = 0 dB, Turbo-TS beamforming can achieve the rate of 10.1 bits/s/Hz, whereas when $N_r \times N_t = 32 \times 128$, the achievable rate can be increased to 14 bits/s/Hz without increasing the number of RF chains.

V. CONCLUSION

In this paper, we have proposed a Turbo-TS beamforming scheme, which consists of two key components: 1) a Turbo-like joint search scheme relying on the iterative information exchange between the BS

and the user and 2) a TS-based precoding/combining scheme utilizing the idea of local search to find the best precoder/combiner in each iteration of Turbo-like joint search with low complexity. Analysis has shown that the complexity of the proposed scheme is linear with N_t^{RF} and N_r^{RF} , and it is independent of B_t^{RF} and B_r^{RF} , which can considerably reduce the complexity of conventional schemes. Simulation results have verified the near-optimal performance of the proposed Turbo-TS beamforming. Our further work will focus on extending the proposed Turbo-TS beamforming to the multiuser scenario.

REFERENCES

- [1] W. Roh *et al.*, "Millimeter-wave beamforming as an enabling technology for 5G cellular communications: Theoretical feasibility and prototype results," *IEEE Commun. Mag.*, vol. 52, no. 2, pp. 106–113, Feb. 2014.
- [2] T. L. Marzetta, "Noncooperative cellular wireless with unlimited numbers of base station antennas," *IEEE Trans. Wireless Commun.*, vol. 9, no. 11, pp. 3590–3600, Nov. 2010.
- [3] S. Han, C.-L. I, Z. Xu, and C. Rowell, "Large-scale antenna systems with hybrid precoding analog and digital beamforming for millimeter wave 5G," *IEEE Commun. Mag.*, vol. 53, no. 1, pp. 186–194, Jan. 2015.
- [4] T. E. Bogale and L. B. Le, "Beamforming for multiuser massive MIMO systems: Digital versus hybrid analog–digital," in *Proc. IEEE GLOBECOM*, Dec. 2014, pp. 10–12.
- [5] X. Zhang, A. F. Molisch, and S.-Y. Kung, "Variable-phase-shift-based RF-baseband codesign for MIMO antenna selection," *IEEE Trans. Signal Process.*, vol. 53, no. 11, pp. 4091–4103, Nov. 2005.
- [6] E. Zhang and C. Huang, "On achieving optimal rate of digital precoder by RF-baseband codesign for MIMO systems," in *Proc. IEEE VTC Fall*, Sep. 2014, pp. 1–5.
- [7] T. E. Bogale, L. B. Le, and A. Haghighat, "Hybrid analog–digital beamforming: How many RF chains and phase shifters do we need?" *arXiv preprint arXiv:1410.2609*, 2014.
- [8] T. Kim *et al.*, "Tens of Gbps support with mmWave beamforming systems for next generation communications," in *Proc. IEEE GLOBECOM*, Dec. 2013, pp. 3685–3690.
- [9] J. Wang *et al.*, "Beam codebook based beamforming protocol for multi-Gbps millimeter-wave WPAN systems," *IEEE J. Sel. Areas Commun.*, vol. 27, no. 8, pp. 1390–1399, Oct. 2009.
- [10] C. Cordeiro, D. Akhmetov, and M. Park, "IEEE 802.11 ad: Introduction and performance evaluation of the first multi-Gbps WiFi technology," in *Proc. ACM Int. Workshop mmWave Commun.*, 2010, pp. 3–8.
- [11] S. Hur *et al.*, "Millimeter wave beamforming for wireless backhaul and access in small cell networks," *IEEE Trans. Commun.*, vol. 61, no. 10, pp. 4391–4403, Oct. 2013.
- [12] F. Glover, "Tabu search—Part I," *ORSA J. Comput.*, vol. 1, no. 3, pp. 190–206, 1989.
- [13] O. El Ayach, S. Rajagopal, S. Abu-Surra, Z. Pi, and R. Heath, "Spatially sparse precoding in millimeter wave MIMO systems," *IEEE Trans. Wireless Commun.*, vol. 13, no. 3, pp. 1499–1513, Mar. 2014.
- [14] L. Dai *et al.*, "Low-complexity soft-output signal detection based on Gauss–Seidel method for uplink multi-user large-scale MIMO systems," *IEEE Trans. Veh. Technol.*, vol. 64, no. 10, pp. 4839–4845, Oct. 2015.
- [15] Z. Pi and F. Khan, "An introduction to millimeter-wave mobile broadband systems," *IEEE Commun. Mag.*, vol. 49, no. 6, pp. 101–107, Jun. 2011.
- [16] L. Wei, R. Q. Hu, Y. Qian, and G. Wu, "Key elements to enable millimeter wave communications for 5G wireless systems," *IEEE Wireless Commun.*, vol. 21, no. 6, pp. 136–143, Dec. 2014.
- [17] L. Dai, Z. Wang, and Z. Yang, "Spectrally efficient time–frequency training OFDM for mobile large-scale MIMO systems," *IEEE J. Sel. Areas Commun.*, vol. 31, no. 2, pp. 251–263, Feb. 2013.
- [18] Z. Gao, L. Dai, and Z. Wang, "Structured compressive sensing based superimposed pilot design in downlink large-scale MIMO systems," *Electron. Lett.*, vol. 50, no. 12, pp. 896–898, Jun. 2014.
- [19] O. El Ayach, R. Heath, S. Abu-Surra, S. Rajagopal, and Z. Pi, "The capacity optimality of beam steering in large millimeter wave MIMO systems," in *Proc. SPAWC Workshops*, 2013, pp. 100–104.

A Bivariate κ - μ Distribution

Mirko Alberto Gomez Villavicencio,
Rausley Adriano Amaral de Souza, *Member, IEEE*,
Geordan Caldeira de Souza, and
Michel Daoud Yacoub, *Member, IEEE*

Abstract—In this paper, a bivariate κ - μ model is presented. Exact expressions for the 1) joint probability density function, the 2) joint cumulative distribution function, 3) joint arbitrary moments, and the 4) normalized envelope correlation coefficient are derived. The joint statistics are given in terms of their respective parameters (κ_1, μ_1) and (κ_2, μ_2) , with $\mu_1 = \mu_2 = \mu > 0$ and arbitrary $\kappa_1 > 0$ and $\kappa_2 > 0$. The parameter describing the correlation between κ - μ fading channels is then written in terms of the physical instances known to affect it in a wireless medium, namely, Doppler shift, the separation distance between two reception points, frequency, and delay spread. As an application example, the outage probability of a dual-branch selection-combining scheme is presented. The effect of correlation in the various aspects of system performance is then investigated. The validity of the analytical results is supported by reducing them to particular cases, for which results are available in the literature, and by means of simulation for the general cases.

Index Terms— κ - μ distribution, bivariate distribution, correlation, fading channel, outage probability, selection combining (SC).

I. INTRODUCTION

The κ - μ fading model describes a fading scenario in which the radio channel exhibits clusters of multipath and dominant components in each cluster [1]. It is characterized by two physical parameters, namely, $\kappa > 0$ and $\mu > 0$. The parameter κ corresponds to the ratio between the total power of the dominant components and the total power of the scattered waves. The parameter μ is related to the number of multipath clusters. The κ - μ fading model contains, as special cases, 1) Nakagami- m , obtained from it as $\kappa \rightarrow 0$ with $\mu = m$ (where m is the Nakagami parameter), and 2) Rice, obtained from it with $\mu = 1$ and $\kappa = k$ (where k is the Rice parameter). Of course, semi-Gaussian and Rayleigh are also special cases of it, because they are special cases of Nakagami- m and Rice.

The κ - μ fading scenario has been explored in a wide range of applications. The usefulness of the κ - μ channel has been recognized in practical situations, and its statistics have been investigated in different environments. In [1] itself, the κ - μ distribution was shown to yield the best fit to data collected in field trials whenever dominant components were present, both for indoor and outdoor environments, for signals

Manuscript received December 10, 2014; revised June 19, 2015; accepted July 23, 2015. Date of publication July 28, 2015; date of current version July 14, 2016. This work was supported in part by Finep, with resources from Funttel, under Grant 01.14.0231.00, through the Radiocommunication Reference Center (Centro de Referência em Radiocomunicações—CRR) project of the National Institute of Telecommunications (Instituto Nacional de Telecomunicações—Inatel), Brazil. The review of this paper was coordinated by Dr. D. W. Matolak.

M. A. G. Villavicencio and M. D. Yacoub are with the Wireless Technology Laboratory (WissTek), Department of Communications (DECOM), School of Electrical and Computer Engineering (FEEC), State University of Campinas (UNICAMP), 13083-852 Campinas, Brazil (e-mail: mirkoalberto2@hotmail.com; michel@wisstek.org).

R. A. A. de Souza and G. C. de Souza are with the National Institute of Telecommunications (Inatel), 37540-000 Santa Rita do Sapucaí, Brazil (e-mail: rausley@inatel.br; geordancal@yahoo.com.br).

Color versions of one or more of the figures in this paper are available online at <http://ieeexplore.ieee.org>.

Digital Object Identifier 10.1109/TVT.2015.2462295